Catalysis of cis/trans isomerization in native HIV-1 capsid by human cyclophilin A

Daryl A. Bosco*, Elan Z. Eisenmesser*, Susan Pochapsky*, Wesley I. Sundquist†, and Dorothee Kern*‡

*Department of Biochemistry, Brandeis University, Waltham, MA 02454

Communicated by Alfred G. Redfield, Brandeis University, Waltham, MA, February 20, 2002 (received for review December 12, 2001)

Packaging of cyclophilin A (CypA) into HIV-1 virions is essential for efficient replication; however, the reason for this is unknown. Incorporation is mediated through binding to the Gly-89–Pro-90 peptide bond of the N-terminal domain of HIV-1 capsid (CA^N). Despite the fact that CypA is a peptidyl-prolyl cis/trans isomerase, catalytic activity on CA^N has not been observed previously. We show here, using NMR exchange spectroscopy, that CypA does not only bind to CA^N but also catalyzes efficiently the cis/trans isomerization of the Gly-89–Pro-90 peptide bond. In addition, conformational changes in CA^N distal to the CypA binding loop are observed on CypA binding and catalysis. The results provide experimental evidence for efficient CypA catalysis on a natively folded and biologically relevant protein substrate.

An interaction between the HIV-1 Gag-encoded capsid (CA) protein and the prolyl isomerase cyclophilin A (CypA) is required for efficient HIV-1 replication (1). As a result of this interaction, CypA is packaged into HIV-1 virions during viral replication at a molar ratio of 1:10 CypA/CA (2–4). CypA is thought to be involved in an early step of HIV-1 replication (5, 6); however, its precise role has not been determined.

CypA belongs to the highly conserved cyclophilin family, members of which are abundantly expressed within many tissue types in both eukaryotic and prokaryotic organisms (7). Cyclophilins are peptidyl prolyl cis/trans isomerases (PPIases) (8, 9) that catalyze the cis/trans isomerization of prolyl peptide bonds (Xaa-Pro), where Xaa can be any amino acid. The cis/trans isomerization by CypA has been extensively characterized using test peptides *in vitro* (8, 10–12). Despite the ubiquitous nature of PPIases, the biological significance of their isomerase activity *in vivo* remains elusive and controversial (13–15). *In vitro* evidence for isomerase activity exists mainly with respect to the acceleration of proline-limited steps in protein folding (7, 16). However, *in vivo* evidence for this activity is sparse (16). An example of a putative folding catalyst is the trigger factor, a ribosome-associated prolyl isomerase that binds nascent polypeptide chains during protein synthesis (17, 18). Human CypA, a cytosolic isomerase, initially gained recognition when it was found to be the target of the immunosuppressive drug cyclosporin A (CsA) (19, 20). The inhibition of PPIase activity by CsA is not related to its immunosuppressive role. Instead, the CypA/CsA complex inhibits the phosphatase calcineurin (21), which in turn suppresses T cell activation.

CypA binds to the Gly-89–Pro-90 (G89-P90) prolyl peptide bond located in a flexible loop within the N-terminal domain of CA (CA^N) (22, 23). The CA^N/CypA interface is formed exclusively through the CA loop sequence Pro-85–Pro-93 (22, 24). The significance of the CA/CypA interaction for HIV-1 virulence has eluded the field for almost a decade. Mutation of either G89 or P90, or addition of CsA, prevents CypA packaging into HIV-1 virions (3, 25), leading to the formation of noninfectious particles. Structural studies of CA^N by NMR revealed that only the G89-P90 peptide bond exists in both a cis (14%) and trans (86%) conformation (23). Interestingly, only a few proteins are known to exhibit such conformational heterogeneity for a prolyl peptide bond in the folded state (ref. 26 and references therein) and, thus far, catalysis of those prolyl peptide bonds by PPIases could not be detected when assayed (27). An intriguing hypothesis for the role of CypA in HIV-1 virulence is that it catalyzes cis/trans isomerization about G89-P90 in CA^N, resulting in a conformational change necessary for CA core disassembly (23). However, because only the trans conformation of G89-P90 is bound to CypA in the CA^N/CypA cocrystal structure, a general view is that CypA most likely plays a chaperone role rather than a catalytic role in HIV-1 virulence (28–30). Here, we present direct experimental evidence for CypA catalysis of the isomerization about the G89-P90 peptide bond in CA^N. To our knowledge, there is no previous direct evidence of CypA isomerase activity on a folded, biologically relevant protein substrate. In addition, we observe chemical shift changes for CA^N residues distal from the CypA binding loop upon CypA wild-type ($CypA^{WT}$) and $CypA^{R55A}$ binding that are indicative of conformational changes not predicted by the CA^N/CypA cocrystal structure (22). The results discussed herein suggest that CypA may have a catalytic role in HIV-1 replication.

Materials and Methods

Protein Purification and Sample Preparation. Vectors for expressing human CypA and CA^N (1–146) have been described (24). $CypA^{R55A}$ was constructed using a quick-change protocol from Stratagene. Proteins were expressed in BL21 (DE3) *Escherichia coli* cells, induced with 1 mM isopropyl β-D-thiogalactoside (IPTG), and harvested after 3 h. Uniformly, ^{15}N-labeled CA^N was grown in M9 minimal media supplemented with $^{15}NH_4Cl$. CypA was purified using an S-Sepharose column equilibrated with 25 mM Mes (pH 6.1)/5 mM β-mercaptoethanol, followed by a QP-Sepharose column equilibrated with 50 mM Tris (pH 6.8)/5 mM β-mercaptoethanol. CypA activity was measured by the coupled chymotrypsin assay (8). CA^N was purified using an S-Sepharose column equilibrated with 100 mM citric acid (pH 4.5)/1 mM DTT, followed by a QP-Sepharose column equilibrated with 75 mM Tris (pH 8.0)/1 mM DTT. Peaks containing CA^N were collected from the flow through. Finally, the buffer of each protein solution was exchanged to 50 mM Na_2HPO_4 (pH 6.5)/1 mM DTT containing 10% D_2O.

NMR samples for ^1H-^{15}N heteronuclear exchange and three-dimensional (3D) ^{15}N edited nuclear Overhauser effect spectroscopy (NOESY)–heteronuclear single quantum coherence (HSQC) experiments were prepared with a molecular ratio of 12:1 (CA^N/CypA). Samples inhibited by CsA (Sigma–Aldrich) were incubated overnight in the presence of excess CsA. For the titration of ^{15}N CA^N with unlabeled $CypA^{WT}$ and $CypA^{R55A}$, a

Abbreviations: CypA; cyclophilin A; CA^N, capsid N-terminal domain; CsA, cyclosporin A; PPIase, peptidyl prolyl cis/trans isomerase; NOESY, nuclear Overhauser effect spectroscopy; HSQC, heteronuclear single quantum coherence; 3D, three-dimensional; G89-P90, Gly-89–Pro-90.

†Present address: Department of Biochemistry, University of Utah, Salt Lake City, UT 84132.

‡To whom reprint requests should be addressed at: Department of Biochemistry, Brandeis University, 415 South Street, Waltham, MA 02454. E-mail: dkern@brandeis.edu.

The publication costs of this article were defrayed in part by page charge payment. This article must therefore be hereby marked "*advertisement*" in accordance with 18 U.S.C. §1734 solely to indicate this fact.

BIOCHEMISTRY

series of titration points were collected ranging from 1:12 CypA/CA^N to 6:1.

NMR Experiments. Two-dimensional (2D) ^1H-^{15}N heteronuclear exchange (31), 3D ^{15}N edited NOESY-HSQC (32), and transverse relaxation-optimized spectroscopy (TROSY)-HSQC (33) spectra were collected on Varian INOVA 600 MHz and 500 MHz spectrometers at 25°C. All NMR spectra were processed with NMRPipe (34). The assignments for free CA^N were provided by M. Summers (23). The CypA catalyzed exchange rate could be determined from the 3D ^{15}N-edited NOESY-HSQC according to ref. 35, because the longitudinal relaxation times for the cis and trans isomer were measured to be equal. ANSIG software (36) was used to compare spectra of ^{15}N-labeled CA^N in the absence and presence of unlabeled CypA. The chemical shift differences between the amide signals of CA^N alone and in the presence of saturating CypA were calculated as follows:

$$\Delta\omega = \sqrt{((\Delta^1H)^2 + (\Delta^{15}N)^2)},$$

where Δ^1H and $\Delta^{15}N$ are the chemicals shift differences in the proton and nitrogen dimensions, respectively.

Results

Catalysis of Cis/Trans Isomerization of the G89-P90 Peptide Bond by CypA. NMR exchange spectroscopy was used to detect catalysis of cis/trans isomerization in CA^N by CypA. This technique identifies conformational exchange processes in a time regime of about 10^{-1} to 10 s between nuclei with different chemical shifts (37). In contrast to most spectroscopic methods, NMR can be used to measure dynamics under steady state or equilibrium conditions, making NMR exchange spectroscopy a powerful tool for analyzing the reversible cis/trans isomerization (11, 12). As previously shown, separate resonance signals can be observed for the cis (14%) and trans (86%) conformation of several amide resonances in close proximity to the G89-P90 peptide bond in CA^N (23), because each conformation resides in distinct chemical environments, and because cis/trans isomerization is slow on the NMR time scale (rate constant of exchange, $k_{ex} < 0.1\ s^{-1}$).

To detect catalysis of cis/trans interconversion by CypA, we performed 2D ^1H-^{15}N heteronuclear exchange experiments (31) on a uniformly ^{15}N-labeled CA^N sample in the absence and presence of catalytic amounts of unlabeled CypA (Fig. 1). Because the uncatalyzed isomerization rate is within the slow-time-scale regime, only the individual peaks (auto peaks) for the cis and trans conformer are observed in the absence of CypA. Addition of catalytic amounts of CypA results in the appearance of exchange peaks connecting G89 cis and trans auto peaks (Fig. 1 *B* and *C*). These results show that cis/trans isomerization about the G89-P90 peptide bond is efficiently catalyzed by CypA. Because of peak overlap, only one exchange peak is completely resolved in the exchange spectrum (Fig. 1 *B* and *C*). Exchange peaks are not observed after inhibition of the isomerase activity by CsA (Fig. 1*D*), or when the catalytically inactive $CypA^{R55A}$ mutant is used in place of $CypA^{WT}$ (data not shown), thus implicating CypA catalysis as the cause for these exchange peaks. These data provide direct evidence that CypA catalyzes the cis/trans isomerization about the G89-P90 peptide bond in native CA^N.

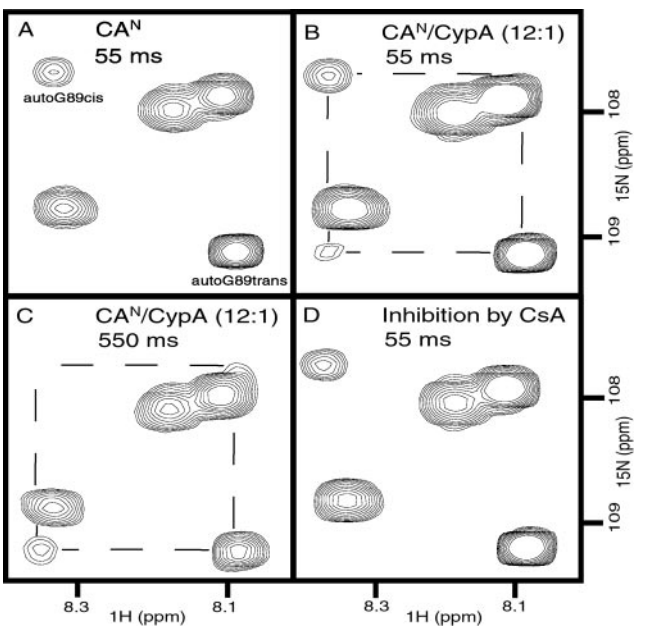

Fig. 1. CypA catalysis of cis/trans isomerization at G89-P90 in folded CA^N. Expansion of ^1H-^{15}N heteronuclear exchange spectra showing the amide signal of G89 for the trans and cis isomer, respectively. Chemical exchange between the cis and trans conformation of G89-P90 is slow in the absence of CypA (*A*) and is accelerated in the presence of catalytic amounts of CypA, as indicated by the appearance of exchange peaks between the cis and the trans auto peaks (*B* and *C*). The intensity of the exchange peak increases with longer mixing time and concurrently the less abundant cis auto peak decreases because of additional loss in magnetization from chemical exchange and longitudinal relaxation (*C*). Inhibition of isomerase activity by CsA results in a loss of the exchange peaks (*D*). The mixing times used in NMR experiments are indicated.

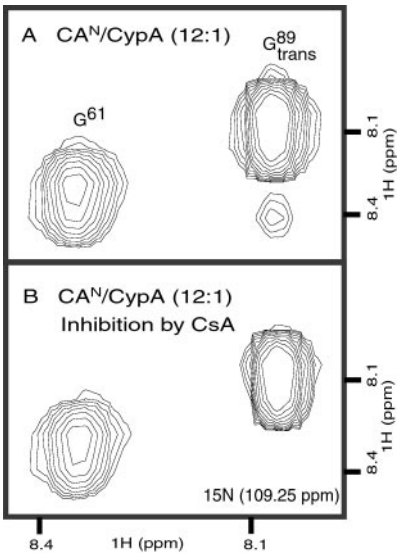

Fig. 2. Quantification of CypA catalysis on CA^N and inhibition by CsA. $^1H/^1H$ plane of a 3D ^{15}N-edited NOESY-HSQC shows the diagonal peak of amide $G89_{trans}$ at 8.0 (^1H) and 109.3 ppm (^{15}N). (*A*) An off-diagonal exchange peak between the amide proton of G89 in the trans and cis conformation is evidence for CypA catalysis and its intensity was used to calculate a cis/trans isomerization rate of $10 \pm 5\ s^{-1}$. (*B*) Addition of excess CsA to sample (*A*) results in a loss of the exchange peak because of inhibition of isomerase activity. Spectrum *B* is identical to a spectrum of CA^N alone (data not shown).

Quantification of Catalysis. The 2D ^1H-^{15}N heteronuclear exchange experiment results (Fig. 1) are further substantiated by the exchange spectra obtained from a 3D ^{15}N-edited NOESY-HSQC experiment (Fig. 2). A chemical exchange peak at ^1H 8.0, ^1H 8.4, and ^{15}N 109.3 ppm is clearly visible in the presence of catalytic amounts of CypA. From this experiment, the exchange rate is calculated as $10 \pm 5\ s^{-1}$ at 25°C from the ratio of the off-diagonal (exchange) peaks to the diagonal (auto) peaks (35).

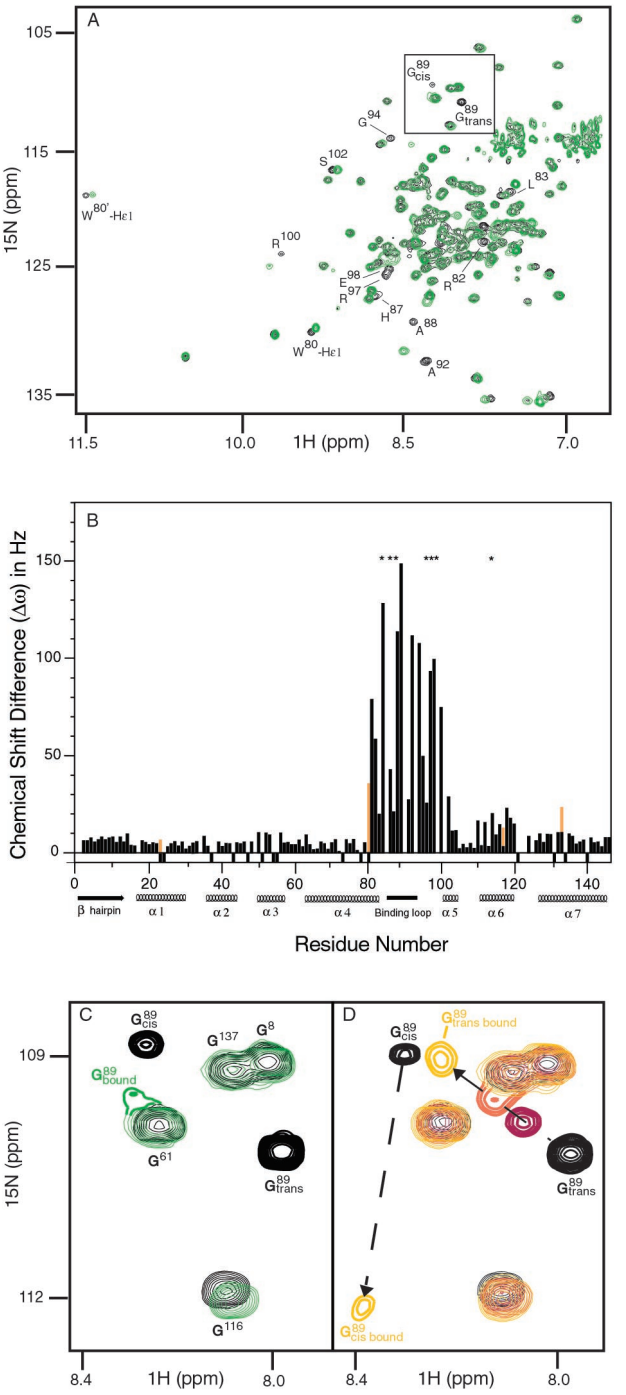

Fig. 3. Characterization of conformational changes in CA^N upon catalysis and/or binding to CypA. (*A*) Comparison of ^1H-^{15}N HSQC-TROSY spectra for CA^N alone (black) and saturated with $CypA^{WT}$ (green) illustrates that residues remote from the CyPA binding loop are affected by CyPA binding and/or catalysis. (*B*) The magnitudes of chemical shift changes for the CA^N amides on complex formation with $CypA^{WT}$ ($\Delta\omega$) are shown as a bar graph. Secondary structure elements and the CypA binding loop (85–93) are labeled. Residues for which $\Delta\omega$ is at least 23 Hz, but which could not be unambiguously determined because of signal overlap, are labeled with an asterisk. Chemical shift changes for the side chain NH of Trp 23, 80, 117, and 133 are shown in orange. An expanded view of the G89 region, highlighted in the full spectrum *A*, is shown in *C* and *D*. At saturating concentrations of $CypA^{WT}$ (CA^N/CypA molar ratio of 1:2), the cis- and trans-bound forms resonate at an average chemical shift because of fast chemical exchange between the two isomers (*C*). Conversely, both the cis and trans conformers of G89 are observed in the enzyme-bound state when the titration is performed with catalytically inactive

Only an upper limit of the uncatalyzed exchange rate can be estimated as 0.1 s^{-1}, consistent with cis/trans isomerization rates of Gly-Pro peptide bonds measured in peptides (38). An apparent acceleration factor of at least 100-fold can be calculated for the CypA concentration used. The exchange peak is not observed after inhibition of the isomerase activity by CsA (Fig. 2*B*). In the absence of CypA, the exchange spectrum is identical to that obtained with CsA (data not shown).

Characterization of the Catalytically Active CA^N/CypA Complex by NMR. In the experiments showing the catalytic action of CypA (described above), only catalytic amounts of CypA were used. We now want to characterize the CA^N/CypA complex and therefore performed NMR experiments at saturating concentrations of CypA. The catalysis of CA^N at G89-P90 by CypA indicates that CypA must bind both the trans and cis conformations of that peptide bond. In contrast, only the trans conformation is seen in the cocrystal structure of the CA^N/CypA complex. In an effort to gain structural information about the active CA^N/CypA complex in solution, a titration of ^{15}N-labeled CA^N with unlabeled CypA was performed. The expected molecular weight of the CA^N/CypA complex is ≈34 kDa. Because of the relatively large molecular weight of the complex, ^1H-^{15}N HSQC-TROSY (33) was used. The TROSY method effectively suppresses transverse (T_2) relaxation, thereby resulting in improved spectral resolution for large macromolecules (39). On addition of increasing amounts of CypA, several amide resonances of CA^N disappear and reappear at different chemical shift locations, indicating slow exchange between free and bound CA^N. This finding is in agreement with a K_D of 15 μM as measured by plasmon resonance biosensor and isothermal titration calorimetry experiments (24). The relatively high affinity between CypA and CA^N enabled us to obtain a 95% saturation of CA^N with CypA (Fig. 3), but prevented us from unambiguously following the chemical shifts. A comparison of free CA^N with the CA^N/CypA complex identified all residues that change in chemical shift in the active complex (Fig. 3 *A* and *B*).

Surprisingly, a number of amide signals in CA^N have altered chemical shifts when bound to and catalyzed by CypA. Based on the CA^N/CypA cocrystal structure, it has been proposed that only residues 85–93 within CA^N are affected by CypA binding (22). However, in addition to the expected chemical shift changes within this flexible binding loop, chemical shift changes also occur within helices α 4, 5, and 6 (Fig. 4). Chemical shift changes are very sensitive markers for conformational changes; however, they do not provide a physical picture of the altered structure.

Dissecting CypA Catalysis and Binding. The minimal reaction scheme for CypA catalyzed cis/trans isomerization of CA^N is shown in Scheme 1. In the presence of CypA, at least four different states of CA^N exist in solution. However, the two CypA-bound forms of CA^N cannot be separated because the cis/trans isomerization in the enzyme-bound states is fast relative to the chemical shift difference between the two states, $\Delta\omega$. Thus, when saturated with $CypA^{WT}$, chemical shift averaging for the enzyme-bound cis and trans conformers of G89 is observed (Fig. 3*C*, Scheme 1). To dissect binding from catalysis, $CypA^{R55A}$ was used with ^{15}N-labeled CA^N in titration experiments similar to those described above for $CypA^{WT}$. It was shown previously that the CypA active site mutation R55A exhibits <1% wild-type

$CypA^{R55A}$ (*D*). The chemical shift changes for $G89_{trans}$ can be followed on titration with $CyPA^{R55A}$ as shown for ratios of CA^N/$CypA^{R55A}$ at 1:1 (red), 1:2 (orange), and 1:6 (yellow). However, for $G89_{cis}$, the bound form is only observed at higher $CyPA^{R55A}$/CA^N ratios in agreement with a higher affinity of the CA^N cis isomer for CypA.

BIOCHEMISTRY

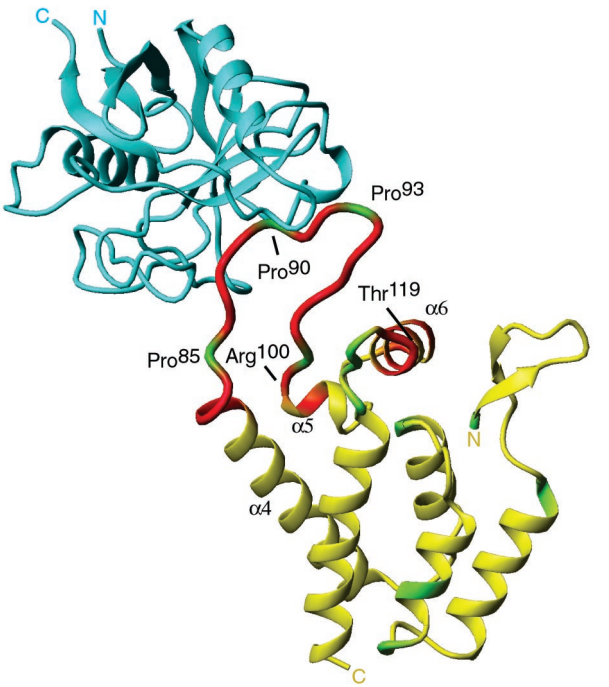

Fig. 4. Identification of residues within CA^N that change in chemical shift on binding and catalysis by CypA (22). CypA (blue) is shown bound to the flexible loop between Pro-85 and Pro-93 of CA^N (yellow). Backbone amides of CA^N that shift on CypA binding by more than 14 Hz are highlighted in red. These residues are not only located within the flexible loop (85–100), but also in α4, α5, and α6. Prolines within CA^N (1–146) are shown in green.

activity (40). As expected, the bound cis and trans conformations of CA^N G89-P90 can now be separately detected in the complex with $CypA^{R55A}$ (Fig. 3*D*). Although the binding events (characterized by K_2 and K_3) do occur for $CypA^{R55A}$ and CA^N, an approximate 100-fold reduction in binding affinity is observed for the mutant protein. An apparent K_D of ≈1.3 mM was calculated based on the NMR titration experiments. The weak binding affinity of $CypA^{R55A}$ for CA^N may explain why this mutant is not incorporated into HIV-1 virions (41, 42). At a molar ratio of 6:1 $CypA^{R55A}/CA^N$, approximately 60% of CA^N is bound to $CypA^{R55A}$, as compared with 95% CA^N bound to CypA at a ratio of 2:1 $CypA/CA^N$.

Overall, the same CA^N amide signals shift when the titration

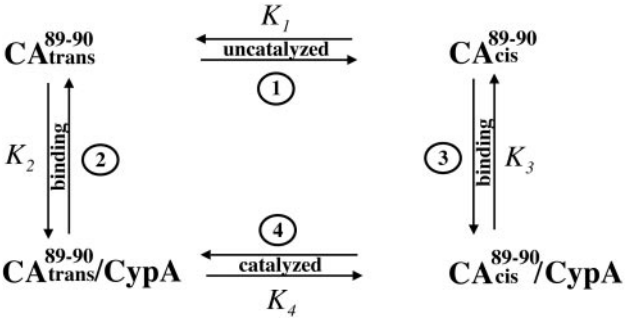

Scheme 1. Four-state model of CypA catalysis on CA^N. The capsid protein exists in two free forms with the G80-P90 peptide bond in the trans (CA^{89-90}_{trans}) and cis conformation (CA^{89-90}_{cis}). Both forms bind to CypA and are interconverted on the enzyme. The rate of uncatalyzed cis/trans isomerization is slow, whereas the catalyzed rate is fast, resulting in an average chemical shift for the two enzyme-bound forms. The relative affinities of the two isomers of CA^N for CypA determine the cis/trans equilibrium constant on the enzyme, K_4.

is performed with $CypA^{WT}$ or with $CypA^{R55A}$. In addition, these CA^N residues shift toward similar chemical shift locations, taking into account that CA^N is only ≈60% saturated by $CypA^{R55A}$ and that there may be minor effects due to the altered chemical environment as a result of the mutation. We therefore conclude that the mutant protein $CypA^{R55A}$ is a suitable model for a qualitative study of the binding events between CA^N and $CypA^{WT}$.

Different chemical shifts are detected for the backbone amides of residues 88, 89, 92, and 95 for the two enzyme-bound forms of CA^N on titration with $CypA^{R55A}$. This observation suggests that the chemical environment for residues in this region is different depending on whether they are bound to CypA in the cis or the trans conformation. For example, the chemical shifts for the cis and trans conformations of A92 are partially overlapped when CA^N is free in solution, but a relatively large chemical shift difference between the cis and trans conformations is observed when bound to $CypA^{R55A}$. For all other amides, no differences in chemical shift between the cis- and trans-bound states could be measured. In addition, the percentage of the cis conformer appears to increase from 14% free in solution to ≈45% when bound to $CypA^{R55A}$ based on the relative signal intensities of the trans- and cis-bound form of CA^N (Fig. 3*D*). This population change corresponds to a 5-fold difference in binding affinity for the two conformers. A higher affinity of the cis conformer is further supported by the fact that the signal of G89 trans shifts with increasing concentrations of $CypA^{R55A}$, whereas the signal of the cis conformer disappears and then reappears (Fig. 3*D*). In other words, exchange between free and CypA-bound CA^N is faster than the chemical shift difference for the trans isomer, but slower for the cis isomer. We note that the equilibrium constant between the CA^N cis and trans isomer when bound to $CypA^{WT}$ (K_4 in Scheme 1) cannot be directly measured based on the binding studies with $CypA^{R55A}$. However, the titration experiments with $CypA^{WT}$ reveal that both isomers have comparable affinities: signals from the cis and trans isomer of CA^N decrease about equally in intensity and later appear at an average chemical shift for the two enzyme-bound isomers during titration with $CypA^{WT}$ (Fig. 3*C*). Furthermore, the average peak position for the two enzyme-bound isomers can be used to approximate the equilibrium constant K_4 for the $CA/CypA^{WT}$ complex. For amides of residues 88, 89, 92, and 95, the average peak is located on a trajectory between the cis and trans-bound form of the $CypA^{R55A}/CA$ complex, but shifted toward the position of the trans-bound form (Figs. 3 *C* and *D*). Because the average peak position is directly determined by the relative populations of the two states, a cis/trans equilibrium constant for the $CA/CypA^{WT}$ complex can be estimated as similar to that of CA^N free in solution (14% cis/86% trans). The change in affinity of the two isomers of CA^N for $CypA^{R55A}$ is likely a direct result of the mutation, because the side chain of R55 within CypA is in hydrogen bond distance to CA^N (22).

Discussion

The detailed mechanism of how cyclophilin A promotes HIV-1 replication is not understood, although several mechanisms have been discussed in recent years (5, 6, 22, 23, 28, 30, 43–45). In light of the CA^N/CypA cocrystal structure showing CA G89-P90 bound exclusively in the trans conformation (22), models depicting CypA as having a chaperone role in HIV-1 virulence have been suggested (28). In fact, a chaperone role has been ascribed to other PPIases (46), and there is speculation as to whether the isomerase activity of PPIases is relevant to their biological function *in vivo* (13, 15, 26). In contrast, our results show that CypA does not simply bind to CA^N, but efficiently catalyzes the cis/trans isomerization about the G89-P90 bond. The finding that CypA can catalyze cis/trans isomerization in a folded

protein may be of more general importance for elucidating the biological mode of action of PPIases on other protein substrates.

CypA Catalysis and HIV-1 Virulence. What are the implications of CypA catalysis for HIV-1 virulence? The present data cannot answer the question of whether the catalytic activity or only pure binding by CypA is responsible for HIV-1 virulence. However, the identification of catalytic action by CypA on CA^N justifies further consideration of a catalytic role for CypA in the enhancement of HIV-1 replication. Dissecting binding from catalysis in the CA/CypA interaction is difficult because mutations rendering CypA catalytically inactive also diminish the ability for Gag to incorporate CypA into HIV-1 virions (41, 42). The fact that the CypA/Gag ratio is substoichiometric in virions is consistent with CypA functioning as a catalyst. Increasing the CypA/Gag ratio to 1:1 ratio actually alters the efficacy of HIV-1 replication (29, 47). Furthermore, the kinetics of HIV-1 replication is largely influenced by the presence of CypA, where replication will still occur in the absence of CypA albeit at a slower rate (1). This finding suggests a kinetic control by CypA rather than an absolute requirement of CypA for replication, again consistent with a catalytic role.

An elegant experiment by Bukovsky *et al.* (48) provided *in vivo* evidence that the CypA binding loop in CA^N is not only responsible for CypA incorporation but is a functional target for CypA. Transfer of the segment between residues 86 and 93 from HIV CA into the corresponding position in simian immunodeficiency virus SIV_{mac} resulted in efficient incorporation of CypA into SIV_{mac}. These SIV_{mac} viruses now showed HIV-1-like sensitivity toward a nonimmunosuppressive CsA analog. The authors further propose that the ability of residues C-terminal to P90 to form a type II turn determines whether CypA is required or will inhibit viral replication. These data support a model where this CA^N type II turn is important for the functional role of CypA in HIV-1 replication, possibly for the destabilization of CA–CA interactions (48), which has also been proposed for the CsA-resistant CA^{A92E} and CA^{G94D} mutants (28, 49, 50). Our results lend support to this model. Interestingly, we observe chemical-shift differences between the cis and trans isomer when bound to $CypA^{R55A}$ for residues within 88–95, indicating that the chemical environment of the type II turn is sensitive to the conformation of the G89-P90 peptide bond. Thus, binding and catalysis by CypA could alter a conformation involving the type II tight turn formed by residues A92 through Q95. In fact, a crucial NOE indicative of a type II turn is absent in the CsA resistant mutant CA^{G94D} (51). Alternatively, the binding event alone between CA and CypA may be sufficient for viral replication. Amide signals of residues distal from the CypA binding loop in CA^N are shifted upon binding to CypA, suggesting that the interaction with CypA may result in conformational changes outside the flexible loop. Some of the observed changes in chemical shift could be a result of a hinge motion about CA^N residues 86–98 (22). It is possible that the conformational changes due to binding could effectively disrupt CA–CA interactions in the virion core, and facilitate CA core disassembly. It remains to be determined whether the catalysis of CA^N by CypA is relevant to HIV-1 virulence *in vivo*.

Catalysis of Cis/Trans Isomerization by Cyclophilin in a Folded Protein. PPIases were originally discovered as enzymes that accelerate folding of certain proteins by catalyzing the rate limiting prolyl cis/trans isomerization (8). Their catalytic activity toward unfolded or partially folded proteins has been extensively studied *in vitro* (7, 15, 16) and has been suggested to be the biological function of the ribosome-associated PPIase trigger factor (17, 18). However, there are a growing number of examples where PPIases are involved in different cellular events (ref. 26 and references therein, refs. 52–55), in which they interact with protein substrates in their folded state. Consequently, the traditional view of PPIase-function needs to be extended to binding and catalysis of prolyl peptide bonds in native substrates.

There are two fundamentally different ways PPIases may control biological activity of a folded protein substrate: (*i*) proline-directed binding or (*ii*) catalysis of cis/trans isomerization (26). For the systems studied to date, the molecular mechanism of PPIase action is poorly understood, and the dissection between the two different modes of action has proven difficult. Moreover, there are a few reports on proteins containing prolyl peptide bonds exhibiting conformational heterogeneity in the folded state (ref. 26 and references therein), a circumstance that most likely reflects the difficulty in detecting native state cis/trans isomerization. In Calbindin D9k, conformational heterogeneity for the G42-P43 peptide was detected (56); however, CypA catalysis was not observed (27).

PPIases have been implicated in the acceleration of cis/trans isomerization for several other proteins, where the conformation of the peptide bond appears to regulate the function (26). For the Ca^{2+}-free form of a C-type mannose binding protein, addition of equimolar amounts of CypA slightly increased the isomerization rate (57). Using 8-anilino-1-naphthalenesulfonic acid (ANS) binding to probe induced-fit conformational changes associated with ATP binding in rabbit muscle adenylate kinase, Sheng *et al.* showed that CypA accelerates ANS binding (58). In both cases, the biological relevance of prolyl isomerization remains unclear. *In vitro* and *in vivo* evidence indicates a possible biological involvement of the FKBP12 PPIase in the inhibition of epidermal growth factor (EGF) (59). A more compelling example of a PPIase that accelerates cis/trans isomerization of prolyl peptide bonds in biologically relevant protein substrates is Pin1. Pin1 is essential for cell cycle regulation *in vivo* via its interaction with the mitosis specific protein cdc25 (60, 61). It is believed that Pin1 catalysis of cis/trans isomerization about phosphorylated Ser-Pro or Thr-Pro peptide bonds in cdc25 and tau, another protein substrate of Pin1, accelerates the dephosphorylation by the phosphatase PP2A (52, 62, 63). For all of the examples described above, the concentration of PPIase required to significantly accelerate cis/trans isomerization of the respective protein substrate was not in catalytic proportions, and rate enhancements were either very small (less than 2-fold; refs. 57 and 58) or the reaction involving the PPIase was completed on the time scale of minutes (52, 59). A recent report shows that substoichiometric amounts of Pin1 can catalyze a conformational change within cdc25 (62).

In contrast to these reports, the catalysis of HIV-1 CA^N by CypA described here is directly visualized, and is found to exhibit an acceleration factor of at least 100-fold when using a substoichiometric $CypA/CA^N$ ratio of 1:12. Taken together, the interaction between CypA and CA^N represents the first example of efficient CypA catalysis on a natively folded and biologically relevant protein substrate. It will be of great interest to further investigate the role of binding versus catalysis for the functions of other PPIases with respect to their natural protein substrates.

Conclusions. The importance of the host protein CypA for HIV-1 virulence has been extensively stated and studied in the last few years. The crystal structure of CA^N in complex with CypA provided a detailed atomic resolution picture of the interface. However, all present data do not explain the mode of action of CypA for virulence. Our results illustrating the catalytic action of CypA on CA call for a more serious consideration of CypA catalysis in HIV-1 replication. Solution NMR enabled not only the detection of catalysis, but also a characterization of both the cis- and trans-bound forms of CA^N. The lack of information about catalysis and the cis-bound form provided by the CA^N/CypA crystal structure is most likely due to trapping one of the existing conformers, a phenomenon often seen in crystallogra-

phy. Furthermore, monitoring the active complex in solution identified residues in CA^N outside the CypA binding loop that are affected by binding. The results shown in this paper, together with the atomic resolution structure of the CA^N/CypA complex, demonstrate how x-ray crystallography and NMR spectroscopy complement each other. Ultimately, additional *in vivo* experiments are needed to elucidate the significance of catalysis and/or binding of the different conformers by CypA for HIV-1 replication.

We thank B. Chamberlin for technical assistance. This work was supported by National Institutes of Health Grants GM62117 (to D.K.) and AI40333 (to W.I.S.), and instrumentation grants awarded by the National Science Foundation and the Keck Foundation (to D.K.).

1. Braaten, D. & Luban, J. (2001) *EMBO J.* **20,** 1300–1309.
2. Luban, J., Bossolt, K. L., Franke, E. K., Kalpana, G. V. & Goff, S. P. (1993) *Cell* **73,** 1067–1078.
3. Franke, E. K., Yuan, H. E. & Luban, J. (1994) *Nature (London)* **372,** 359–362.
4. Thali, M., Bukovsky, A., Kondo, E., Rosenwirth, B., Walsh, C. T., Sodroski, J. & Gottlinger, H. G. (1994) *Nature (London)* **372,** 363–365.
5. Braaten, D., Franke, E. K. & Luban, J. (1996) *J. Virol.* **70,** 3551–3560.
6. Fitzon, T., Leschonsky, B., Bieler, K., Paulus, C., Schroder, J., Wolf, H. & Wagner, R. (2000) *Virology* **268,** 294–307.
7. Gothel, S. F. & Marahiel, M. A. (1999) *Cell Mol. Life Sci.* **55,** 423–436.
8. Fischer, G., Bang, H. & Mech, C. (1984) *Biomed. Biochim. Acta* **43,** 1101–1111.
9. Fischer, G., Wittmann-Liebold, B., Lang, K., Kiefhaber, T. & Schmid, F. X. (1989) *Nature (London)* **337,** 476–478.
10. Harrison, R. K. & Stein, R. L. (1990) *Biochemistry* **29,** 3813–3816.
11. Kern, D., Drakenberg, T., Wikstrom, M., Forsen, S., Bang, H. & Fischer, G. (1993) *FEBS Lett.* **323,** 198–202.
12. Kern, D., Kern, G., Scherer, G., Fischer, G. & Drakenberg, T. (1995) *Biochemistry* **34,** 13594–13602.
13. Schreiber, S. L. & Crabtree, G. R. (1992) *Immunol. Today* **13,** 136–142.
14. Ivery, M. T. (2000) *Med. Res. Rev.* **20,** 452–484.
15. Schiene, C. & Fischer, G. (2000) *Curr. Opin. Struct. Biol.* **10,** 40–45.
16. Schmid, F. X. (1995) *Curr. Biol.* **5,** 993–994.
17. Stoller, G., Rucknagel, K. P., Nierhaus, K. H., Schmid, F. X., Fischer, G. & Rahfeld, J. U. (1995) *EMBO J.* **14,** 4939–4948.
18. Deuerling, E., Schulze-Specking, A., Tomoyasu, T., Mogk, A. & Bukau, B. (1999) *Nature (London)* **400,** 693–696.
19. Handschumacher, R. E., Harding, M. W., Rice, J., Drugge, R. J. & Speicher, D. W. (1984) *Science* **226,** 544–547.
20. Takahashi, N., Hayano, T. & Suzuki, M. (1989) *Nature (London)* **337,** 473–475.
21. Liu, J., Farmer, J. D., Jr., Lane, W. S., Friedman, J., Weissman, I. & Schreiber, S. L. (1991) *Cell* **66,** 807–815.
22. Gamble, T. R., Vajdos, F. F., Yoo, S., Worthylake, D. K., Houseweart, M., Sundquist, W. I. & Hill, C. P. (1996) *Cell* **87,** 1285–1294.
23. Gitti, R. K., Lee, B. M., Walker, J., Summers, M. F., Yoo, S. & Sundquist, W. I. (1996) *Science* **273,** 231–235.
24. Yoo, S., Myszka, D. G., Yeh, C., McMurray, M., Hill, C. P. & Sundquist, W. I. (1997) *J. Mol. Biol.* **269,** 780–795.
25. Braaten, D., Franke, E. K. & Luban, J. (1996) *J. Virol.* **70,** 4220–4227.
26. Fischer, G., Tradler, T. & Zarnt, T. (1998) *FEBS Lett.* **426,** 17–20.
27. Kordel, J., Drakenberg, T., Forsen, S. & Thulin, E. (1990) *FEBS Lett.* **263,** 27–30.
28. Luban, J. (1996) *Cell* **87,** 1157–1159.
29. Yin, L., Braaten, D. & Luban, J. (1998) *J. Virol.* **72,** 6430–6436.
30. Wiegers, K., Rutter, G., Schubert, U., Grattinger, M. & Krausslich, H. G. (1999) *Virology* **257,** 261–274.
31. Farrow, N. A., Zhang, O., Forman-Kay, J. D. & Kay, L. E. (1994) *J. Biomol. NMR* **4,** 727–734.
32. Sattler, M., Schleucher, J. & Griesinger, C. (1999) *Prog. NMR Spectrosc.* **34,** 93–158.
33. Pervushin, K., Riek, R., Wider, G. & Wuthrich, K. (1997) *Proc. Natl. Acad. Sci. USA* **94,** 12366–12371.
34. Delaglio, F., Grzesiek, S., Vuister, G. W., Zhu, G., Pfeifer, J. & Bax, A. (1995) *J. Biomol. NMR* **6,** 277–293.
35. Baine, P. (1986) *Magn. Reson. Chem.* **24,** 304–307.
36. Kraulis, P. J., Domaille, P. J., Campbell-Burk, S. L., Van Aken, T. & Laue, E. D. (1994) *Biochemistry* **33,** 3515–3531.
37. Perrin, C. L. & Dwyer, T. J. (1990) *Chem. Rev.* **90,** 935–967.
38. Wuthrich, C. G. n. K. (1981) *Biopolymers* **20,** 2623–2633.
39. Pervushin, K. (2000) *Q. Rev. Biophys.* **33,** 161–197.
40. Zydowsky, L. D., Etzkorn, F. A., Chang, H. Y., Ferguson, S. B., Stolz, L. A., Ho, S. I. & Walsh, C. T. (1992) *Protein Sci.* **1,** 1092–1099.
41. Braaten, D., Ansari, H. & Luban, J. (1997) *J. Virol.* **71,** 2107–2113.
42. Dorfman, T., Weimann, A., Borsetti, A., Walsh, C. T. & Gottlinger, H. G. (1997) *J. Virol.* **71,** 7110–7113.
43. Endrich, M. M., Gehrig, P. & Gehring, H. (1999) *J. Biol. Chem.* **274,** 5326–5332.
44. Pushkarsky, T., Zybarth, G., Dubrovsky, L., Yurchenko, V., Tang, H., Guo, H., Toole, B., Sherry, B. & Bukrinsky, M. (2001) *Proc. Natl. Acad. Sci. USA* **98,** 6360–6365.
45. Sherry, B., Zybarth, G., Alfano, M., Dubrovsky, L., Mitchell, R., Rich, D., Ulrich, P., Bucala, R., Cerami, A. & Bukrinsky, M. (1998) *Proc. Natl. Acad. Sci. USA* **95,** 1758–1763.
46. Baker, E. K., Colley, N. J. & Zuker, C. S. (1994) *EMBO J.* **13,** 4886–4895.
47. Gross, I., Hohenberg, H., Huckhagel, C. & Krausslich, H. G. (1998) *J. Virol.* **72,** 4798–4810.
48. Bukovsky, A. A., Weimann, A., Accola, M. A. & Gottlinger, H. G. (1997) *Proc. Natl. Acad. Sci. USA* **94,** 10943–10948.
49. Aberham, C., Weber, S. & Phares, W. (1996) *J. Virol.* **70,** 3536–3544.
50. Braaten, D., Aberham, C., Franke, E. K., Yin, L., Phares, W. & Luban, J. (1996) *J. Virol.* **70,** 5170–5176.
51. Campos-Olivas, R. & Summers, M. F. (1999) *Biochemistry* **38,** 10262–10271.
52. Zhou, X. Z., Kops, O., Werner, A., Lu, P. J., Shen, M., Stoller, G., Kullertz, G., Stark, M., Fischer, G. & Lu, K. P. (2000) *Mol. Cell* **6,** 873–883.
53. Gaburjakova, M., Gaburjakova, J., Reiken, S., Huang, F., Marx, S. O., Rosemblit, N. & Marks, A. R. (2001) *J. Biol. Chem.* **276,** 16931–16935.
54. Lee, J. P., Palfrey, H. C., Bindokas, V. P., Ghadge, G. D., Ma, L., Miller, R. J. & Roos, R. P. (1999) *Proc. Natl. Acad. Sci. USA* **96,** 3251–3256.
55. Jin, Z. G., Melaragno, M. G., Liao, D. F., Yan, C., Haendeler, J., Suh, Y. A., Lambeth, J. D. & Berk, B. C. (2000) *Circ. Res.* **87,** 789–796.
56. Chazin, W. J., Kordel, J., Drakenberg, T., Thulin, E., Brodin, P., Grundstrom, T. & Forsen, S. (1989) *Proc. Natl. Acad. Sci. USA* **86,** 2195–2198.
57. Ng, K. K. & Weis, W. I. (1998) *Biochemistry* **37,** 17977–17989.
58. Sheng, X. R., Zhang, H. J., Pan, X. M., Li, X. F. & Zhou, J. M. (1997) *FEBS Lett.* **413,** 429–432.
59. Lopez-Ilasaca, M., Schiene, C., Kullertz, G., Tradler, T., Fischer, G. & Wetzker, R. (1998) *J. Biol. Chem.* **273,** 9430–9434.
60. Lu, K. P., Hanes, S. D. & Hunter, T. (1996) *Nature (London)* **380,** 544–547.
61. Yaffe, M. B., Schutkowski, M., Shen, M., Zhou, X. Z., Stukenberg, P. T., Rahfeld, J. U., Xu, J., Kuang, J., Kirschner, M. W., Fischer, G., *et al.* (1997) *Science* **278,** 1957–1960.
62. Stukenberg, P. T. & Kirschner, M. W. (2001) *Mol. Cell* **7,** 1071–1083.
63. Lu, P. J., Wulf, G., Zhou, X. Z., Davies, P. & Lu, K. P. (1999) *Nature (London)* **399,** 784–788.